

Advanced Microscopy of Microbial Cells

Janus A. J. Haagensen, Birgitte Regenberg and Claus Sternberg

Abstract Growing awareness of heterogeneity in cells of microbial populations has emphasized the importance of advanced microscopy for visualization and understanding of the molecular mechanisms underlying cell-to-cell variation. In this review, we highlight some of the recent advances in confocal microscopy, super-resolution optical microscopy (STED, SIM, PALM) as well as atomic force microscopy and Raman spectroscopy. Using examples of bistability in microbial populations as well as biofilm development and differentiation in bacterial and yeast consortia, we demonstrate the importance of microscopy for visualization of variation between cells in phenotypic traits such as gene expression.

Keywords Advanced microscopy techniques • Single-cell gene expression • Bistability • Biofilm development and differentiation • Bacteria • Yeast

Abbreviations

AFM	Atomic force microscope
AOBS	Acousto-optical beam splitter
AOTF	Acousto-optical tunable filter
CARS	Coherent anti-Stokes Raman spectroscopy
CFP	Cyan fluorescent protein
CLSM	Confocal laser scanning microscope
EPS	Extracellular polymeric substance
FRAP	Fluorescence recovery after photobleaching

J. A. J. Haagensen
Stanford University, The Bio-X Program, Clark Center,
318 Campus Drive, Stanford, CA 94305, USA
e-mail: Haagensen@stanford.edu

B. Regenberg and C. Sternberg (✉)
Department of Systems Biology, Technical University of Denmark,
Building 301, 2800 Kongens Lyngby, Denmark
e-mail: cst@bio.dtu.dk

B. Regenberg
Department of Biology, Molecular Integrative Physiology,
Universitetsparken 13, 2100 Copenhagen, Denmark
e-mail: bregenberg@bio.ku.dk

GFP	Green fluorescent protein
MP	Multi photon
NA	Numerical aperture
PALM	Photo-activated localization microscopy
PE	Polyethylene
PI	Propidium iodide
PMT	Photo multiplier
PP	Polypropylene
PVC	Polyvinyl chloride
SIM	Structured illumination microscopy
SERS	Surface enhanced Raman spectroscopy
STED	Stimulated emission depletion
TERS	Tip enhanced Raman spectroscopy
STORM	Stochastic optical reconstruction microscopy
YFP	Yellow fluorescent protein

Contents

1	Introduction.....	23
2	Advanced Microscopy and Tools	24
2.1	The Standard Confocal Microscope Today	24
2.2	Wide Spectrum (“white”) Lasers	24
2.3	Multi-Photon/Two-Photon Microscopy.....	25
2.4	Super Resolution Confocal Microscopy	26
2.5	Other Microscopy Techniques Surpassing the Diffraction Resolution Limit.....	27
2.6	Atomic Force Microscopy.....	28
2.7	Single-Cell Fluorescent Labeling, Visualization and Physiology.....	29
2.8	Raman Microscopy.....	30
2.9	Presentation and Analysis Software.....	32
3	Bacterial Single-Cell and Biofilm Microscopy, Bistability and Subpopulations	32
3.1	Bistability in <i>B. subtilis</i>	33
3.2	Bimodal Gene Expression and Biofilm Formation.....	35
3.3	Persistence and Bistability in <i>E. coli</i>	37
3.4	Raman Microscopy of Bacterial Cells.....	38
3.5	<i>Pseudomonas aeruginosa</i> Biofilm Development and Differentiating Subpopulations.....	40
4	Yeast Single-cell and Biofilm Microscopy	42
4.1	Cell-to-Cell Variation in Yeast Populations.....	43
4.2	Bistability in Yeasts.....	43
4.3	Microscopy of <i>Candida albicans</i> Biofilm.....	44
4.4	Confocal Microscopy of <i>S. cerevisiae</i> Biofilms on Batch Culture Slides and in Flow Chambers	45
5	Future Perspectives.....	47
	References	48

1 Introduction

While culture or community-based approaches where millions of organisms are studied collectively as a single entity are adequate for general physiological studies, microscopy of single cells and subpopulations has lately been realized as an important and sometimes indispensable tool when a community of apparently homogenous cells is investigated for phenotypic diversity.

The often used assumption when monitoring gene expression in a bacterial population is to consider the population as a uniform pool. However, this will only report average values and never pick up variations between individual single cells. This assumption has been prevailing as analyzing and visualizing single cells in large populations have been difficult or impossible.

Microscopy has been an important method for analysis of microbial cells since Antonie van Leeuwenhoek described amoebae and other microorganisms in the late 1600s. The ‘compound microscope’, i.e., a microscope with more than one lens, was invented almost a century before these first reports of living microorganisms [8]. Development of the microscope has since undergone numerous improvements, where some of the most notable are the invention of the fluorescence microscope [60], the phase contrast principle [150], the electron microscope in 1931 [114], the confocal microscope in 1955 [89], and the atomic force microscope (AFM) in 1986 [15] and derivatives of these.

Today, new technologies provide the possibility to differentiate between subpopulations and to analyze single cells for altered gene expression using advanced microscopy, cell sorting and a growing number of fluorescent reporter tools. An increased awareness of cellular differentiation has emphasized the need for understanding of microbial gene expression and provides a more efficient and direct treatment of bacterial and fungal infections [128, 138]. Furthermore, a better insight into the regulation of differentiation in bacteria and yeasts can lead to a wider application in biotechnology [27].

Microbes are found everywhere from settings in the human host to soil and aquatic environments. They are constantly meeting new environmental conditions and have evolved highly sophisticated abilities to adapt to changes. Several adaptive mechanisms are used by microbial populations to turn on and off genes stochastically in a population of cells while being in the same environment. This approach can ensure that a subpopulation of cells will survive in a situation where life conditions suddenly change (bet-hedging). Bistability is an example of a molecular mechanism that has evolved to diversify the transcriptional program and phenotype of a clonal population within the same environment. Bistability can be described as an inheritable and reversible switch at the level of transcription that does not involve genetic rearrangements or mutations but is rather epigenetic in its nature [27, 35, 39].

In this chapter, we will describe the current state of the art microscopy techniques and use bistability in microbial populations and biofilm development and

differentiation in these as examples of biological properties, which to a large extent has been observed and investigated using advanced microscopy.

2 Advanced Microscopy and Tools

2.1 *The Standard Confocal Microscope Today*

From the time the first confocal microscopes became commercially available, a long range of improvements has been implemented and are now standard: The lasers used in most microscopes have a much improved lifetime compared to early models, and in particular the ruggedness of diode lasers significantly extend the period before replacement is necessary. In addition, this type of laser requires less for the installation environment in terms of power supply and cooling—all factors that lower the running costs. Traditional gas lasers, such as the most common Argon gas laser, has also improved and now provides longer life spans. The detectors of confocal microscopes are traditionally photo-multipliers, PMTs. Their sensitivity largely determines the overall image quality, particularly in conditions of low light intensity. Newer PMTs have improved signal-to-noise ratios, enabling detection of fainter fluorescence signals. The band-pass filters on the emission side has also been improved from the original glass filters, which were placed in the light path manually, over motorized filter wheels to the acousto-coupled beam deflector [42], commonly known as an acousto-optical tunable filter (AOTF). AOTF selectively deflects specific wavelengths out of the light path, leading only the desired emission to the detectors. This technology has been developed into multiline spectral splitters, such as the acousto-optical beam splitter (AOBS) [16], which allows for detection of multiple wavelength ranges simultaneously. An alternative to this is the technology where the light beam is spectrally split by a grate working like a prism, and selected parts of the spectrum are captured by an array of detectors.

Confocal microscopes have been and are widely used in the study of complex microbial communities (biofilms) since the first reports by the Caldwell group in 1992 [21, 85] and onto the present day [97, 103, 148].

2.2 *Wide Spectrum (“white”) Lasers*

Traditional gas lasers can emit light of at most a few, well-defined wavelengths. For instance, the most commonly used laser in confocal microscopy, the Argon gas laser, emits a range of monochromatic wavelengths at 488, 351, 454.6, 457.9, 465.8, 476.5, 496.5, 501.7, 514.5 and 528.7 nm. However, in the standard visible light configuration, the laser is configured to mainly provide 488-nm blue excitation light. Some of the other wavelengths require alteration of the mirror system

to be usable, and some are considerably weaker than the 488-nm line. It is also common that commercial instruments have multiple lasers with different characteristics to enable the use of more fluorophores. Despite multiple simultaneous lasers, the choices of excitation wavelengths are limited. To alleviate this, the super-continuum laser, also known as the “white” laser, has been introduced. The super-continuum laser is a compound laser consisting of a pump laser and a crystal photonic fiber optic. A conventional laser delivers a narrow band laser illumination to the end of the fiber that consists of a bundle of hollow tubes. When passing through the fiber the spectrum is broadened, resulting in a wide spectrum emission. The width of the spectrum depends on the pattern and length of the tube arrangement inside the fiber. The first verified reports of broad spectrum laser light were published already in 1970 [3, 4]. However, it was only after the invention of the hexagonal photonic fiber that the white laser we know today was made useful for practical applications [81]. The technology is currently used for confocal microscopy [18] and stimulated emission depletion (STED) [145–147] (see below). A typical wide spectrum laser used in confocal microscopy has a spectrum covering most of the visible wavelengths, 470–670 nm.

2.3 Multi-Photon/Two-Photon Microscopy

Conventional confocal imaging has its basis in the fluorescence microscope, i.e., the specimen must contain a dye that is fluorescent—an added dye in the form of a chemical, a fluorescent protein expressed by cells in the sample or auto-fluorescence. The sample is illuminated using a laser throughout the entire depth, and fluorescence is emitted from the whole cross section. The emission pinhole will remove most of the fluorescence from all planes except the focal plane. This method is most likely harmful to living cells as all cells are exposed to laser radiation for the duration of the scanning, and the aberrant fluorescence from the layers other than the focal plane *do* in fact contribute to noise in the image.

The two- or multi-photon (MP) principle [51] predicts that when two or more photons hit a fluorophore simultaneously (i.e., within a femtosecond timeframe) the two photons will both contribute to the excitation. In other words, a longer wavelength laser illumination can provide a localized energy pulse corresponding to that of a shorter, more energy-rich wavelength used in a conventional one-photon system. Thus, using infrared laser light, it is possible to excite molecules that require, e.g., blue light for excitation. Since the multi-photon effect only occurs where more photons are precisely in synchronicity, it is possible to exploit this property to narrow the illumination to an extremely small volume. This is used in the two-photon confocal microscope [36]. The MP-confocal microscope gives better vertical (z -)resolution, about 100 nm [96] compared to 5–700 nm for conventional, one-photon confocal microscopy. High-resolution confocal microscopy of relatively thick specimens is possible with MP excitation [95, 96]. The emission pinhole is not necessary, since only objects in a small volume in the focal plane are

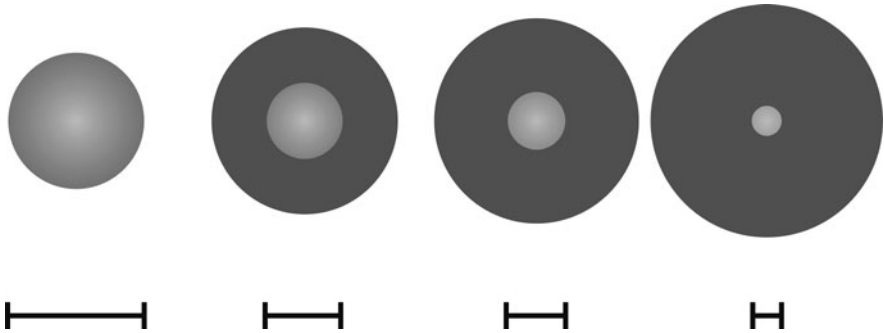


Fig. 1 Stimulated emission depletion (STED) microscopy. Without STED the fluorescence emission light (*light grey*) produces a light spot, which cannot be localized to a better resolution than predicted by Abbe. By application of a ring-shaped STED laser light (*dark grey*) that extinguishes parts of the fluorescence from the sample, the effective resolution is improved. By increasing the STED laser effect, the resolution improves accordingly, as indicated by the *size indicator bars*

excited by more than one photon at a time, the remainder of the specimen only experiences long wavelength light with less detrimental effects (both for cytotoxicity and bleaching). However, since the light flux is very high in the small volume that is excited, cell damage can occur if care is not taken to protect the exposed cells [67]. MP microscopy in life sciences was reviewed by König [83].

2.4 Super Resolution Confocal Microscopy

Ernst Abbe (1840–1905) determined the theoretical optical resolution as $d = \lambda / 2\text{NA}$, where λ is the wavelength and NA is the numerical aperture of the objective [1]. Using visible light, this means that the practical horizontal resolution (the distance to resolve two objects) is 200–250 nm. While this is sufficient for many purposes, analysis of sub-cellular structures, surface components and appendages is rarely possible. Electron microscopy and atomic force microscopy (see below) have several-fold improved resolution but have other shortcomings; e.g., electron microscopy usually requires the sample to be fixed, dried and dyed with metal dyes, whereas atomic force microscopy is restricted to analysis of the top surface of structures with little variation in height. The optical microscope is superior since it allows scrutiny of living, wet samples in three dimensions.

A number of methods now exist to circumvent the law of Abbe, either as a physical, on-line method or as a computational reconstruction from several interlaced images. Probably the most prominent high-resolution technology is STED [40, 57, 63, 79]. In STED the sample is illuminated by two tightly synchronized light pulses. The fluorophore is excited with a pulsed excitation beam, e.g., 640 nm, which causes the sample to emit light (Fig. 1). Without STED, the

emitted light will have a diffraction limit that in part is determined by Abbe's equation. STED adds an additional light pulse at, e.g., 730–780 nm, which is doughnut shaped with a dark center. The wavelength of the STED illumination does not excite the fluorophore—rather it causes the already excited molecules to return to the ground state without emitting light. The result is that fluorescence is only emitted from the dark center, the size of which is determined by the laser power of the STED light, increasing the effective resolution to this center area.

Instrument development platforms have reached a resolution of 5.8 nm [111], while commercial instruments typically will have a lower effective resolution. The first generation STED microscopes were limited in the number of fluorescent dyes that could be employed since the laser configuration required was limited to 640 nm excitation and 730–780 nm depletion. Using lasers with tunable excitation wavelengths, the STED technology has broadened the versatility of the instrument. Using the continuous wave laser or super-continuum lasers, it is possible to utilize commonly used markers such as green fluorescent protein (GFP) with a resolution of 29–60 nm [61, 145–147].

2.5 Other Microscopy Techniques Surpassing the Diffraction Resolution Limit

Computational treatment of images after acquisition demonstrate other methods for rendering of images with sub-diffraction resolution. Three such methods have been commercialized, the stochastic optical reconstruction microscopy (STORM), photo-activated localization microscopy (PALM) and structured illumination microscopy (SIM).

STORM is based on sequential excitation of photo-switchable fluorophores in a sample followed by reconstruction of a high-resolution image from a series (sometimes hundreds or thousands) of images of the same field of view [68, 115]. The principle of STORM is that only a fraction of the fluorophores are excited at any time in the sample, which then is recorded by the microscope. A quenching light pulse extinguishes the fluorophores and excites another set of dye spots in the sample. By changing the position that is illuminated or quenched, it is possible to record a fine map of the position of the fluorescent molecules. Using computer programs, this information can be converted into an image with in principle unlimited resolution [115], but mechanical limitations give an effective resolution in the range of 20 nm. PALM is an independently developed technique using the same principle as STORM [13, 64, 104, 122]. One prominent feature of this method for resolution improvement is that that in principle standard microscopy equipment and a low cost laser are all that is required of the hardware, although advanced software is needed for the post-recording image manipulation. STORM and PALM have been used for 3D imaging [68, 76, 105, 123, 137] and multicolor imaging [10, 118, 122].

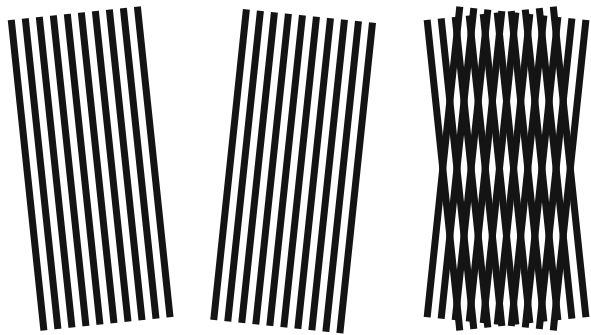
SIM uses the principle of interlaced information from structured illumination by very high-resolution patterns that are projected onto the fluorescent sample. When two patterns are overlaid, these images result in a moiré fringe with a lower resolution. Figure 2 demonstrates how two idealized high-resolution patterns result in a moiré fringe (here perceived as horizontal lines) with lower resolution (spacing) than the original patterns. In the SIM one of the patterns is comprised of the structure in the sample (the distribution of fluorescent dye) and the overlaying pattern of the illumination pattern. Using multiple images recorded with different illumination angles and mathematical processing, it is possible to reconstruct an image with resolution corresponding to the resolution of the illumination pattern.

This method gives approximately a two-fold improvement in resolution compared to the diffraction limit determined by Abbe [48]. A recent extension of this technique, saturated SIM (SSIM), has further moved the resolution limit. SSIM utilizes nonlinear patterned excitation of fluorescent samples and the image reconstruction techniques of SIM to achieve in principle unlimited resolution, while practical experimental setups have yielded a resolution of roughly 50 nm, or four times that of standard microscopy [49, 62]. Due to the requirement for overlay of several sequentially recorded images, SIM and SSIM are less well suited for imaging of living cells, but a recent report has demonstrated SIM of slowly moving cells [66].

2.6 Atomic Force Microscopy

Atomic force microscopy is a non-optical surface scanning method in which a tip (probe) at the end of a flexible cantilever is transversing a structured surface. The AFM can operate in several different modes. The two most commonly used for imaging are contact mode and tapping mode, or dynamic mode. In contact mode, the tip is dragged across the surface and irregularities on the surface cause the cantilever, which is carrying the tip, to bend up and down. A laser is recording the bend, which can be directly correlated to the topology of the surface. In tapping mode an oscillating frequency is applied to the cantilever, making the tip move up

Fig. 2 Structured illumination microscopy (SIM). In consecutive scans, a patterned illumination is applied to the sample. The illumination pattern in combination with the fluorescence pattern in the sample (*symbolized by the lines in the middle panel*) result in a moiré pattern that can be the basis for computer-assisted image reconstruction



and down towards the surface. In tapping mode the tip is subjected to a combination of attractive and repulsive forces, which influence the amplitude of the oscillation. A feedback loop corrects the distance between the cantilever and the sample by piezo-electrical actuators (moving the stage or the cantilever-mount) to bring the amplitude back to the initial state (Fig. 3). The required correction can be correlated to the distance between the tip and sample at a specific position and then converted to a height (3D) image of the surface when the tip is moved across the sample.

The AFM has atomic resolution on crystalline surfaces and nanometer resolution on other surfaces. It can be operated in liquids and gaseous environments. Applications of atomic force microscopy in biological research began in the early 1990s [50, 86, 117, 133]. As the AFM became more integrated in life science research, this new tool provided a new approach for the examination of biomolecules including proteins [55, 107, 117], DNA [56, 86, 134] and highly topographic samples, such as bacterial [5, 17, 19, 22, 112] and yeast cells [44, 77] at nanoscale resolution. Most importantly, samples could be imaged in physiological relevant media, and in the case of bacteria and mammalian cells living cells could be imaged in their native environment. While the AFM provides imaging with extreme resolution, it does only facilitate analysis of surfaces that are accessible from above; hence, it is not suitable for analysis of intercellular processes.

2.7 Single-Cell Fluorescent Labeling, Visualization and Physiology

Several microscopic methods require that cells are fluorescent. Consequently, it is important to have tools available for staining or marking investigated cells with specific fluorescent labels.

Recently, there has been a development of fluorescent stains, such as the Syto stains (Invitrogen, Carlsbad, CA), that efficiently, although unspecifically, can

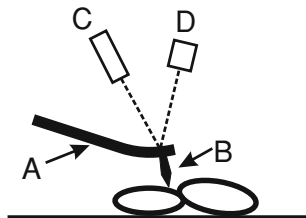


Fig. 3 Atomic force microscopy. The sample is scanned by a moving tip (b), which is attached to a flexible cantilever (a). The deflection of the cantilever is recorded by using a laser (c) illuminating a spot on the back of the cantilever. The position of the spot is recorded by a photomultiplier (d), and a feedback loop moves the cantilever or the sample to return the deflection to a neutral state (as determined by the location of the laser spot)

stain cells. Combinations of stains with different excitation and emission wavelengths are available for possible use together with reporter gene constructs. Using Syto9-labeled cells in combination with propidium iodide (PI), it is possible to specifically determine living and dead cells in a population. The dye Syto9 will mark all cells green, while it is generally assumed that only cells with a damaged membrane integrity will be stained by the red PI dye, indicating dead cells. PI will reduce Syto9 in dead cells, making them only fluoresce red. Recent results suggest that propidium iodide might be of limited use as a cell viability indicator in some settings and for some strains. Therefore, it is important for each species and environment to calibrate the concentration of dye [91, 121].

As an alternative to direct staining, a common method used today is to modify the cells of interest genetically by chromosomal tagging with a gene cassette encoding a fluorescent protein or by plasmid introduction. In this way GFP (green), RFP (red), CFP (cyan) and YFP (yellow) have been successfully introduced into many different cell types. GFP-tagged cells can substitute the use of Syto9 in the live/dead assay described above.

Fluorescent tagging can be used as simple labeling to verify and visualize the location of several species in a mixed community. By selecting suitable variants of fluorescent protein genes and promoters, this kind of tagging can be used for monitoring gene expression in specific cells. This way metabolic/physiological activity has been determined in biofilms by introducing constructs encoding for GFP derivatives with a short half-life, placed under transcriptional control of a ribosomal promoter. Cells that have a high activity will show as bright green, whereas cells with low or no activity show little or no fluorescence [130].

2.8 Raman Microscopy

Raman spectroscopy is a method that can produce a fingerprint of the chemical composition of materials in a cell based on Raman scattering of the molecules in the materials. Molecules that are hit by an incoming photon can either absorb or scatter the light, or not interact at all with the light. The scattered light will primarily have the same wavelength as the incoming light, whereas a very small fraction ($1 \text{ per } 10^6\text{--}10^8$ photons) will have a different, higher or lower, wavelength due to vibrational or rotational effects in the molecule: When a photon interacts with the electron cloud and bonds in a molecule, it can excite it to a more energetic state. Most photons excite a molecule to a higher virtual energy state from a relaxed state. When the molecule returns to the relaxed state, energy of the same magnitude (and hence photons with the same wavelength) as the excitation energy is released. This is called Rayleigh scattering (Fig. 4).

Occasionally, however, the molecule may be excited to the higher virtual energy state and return to an energy state that has a higher level than the relaxed state, releasing less energy than the excitation photon. This will then result in a scattering photon with less energy, i.e., longer wavelength, called Stokes

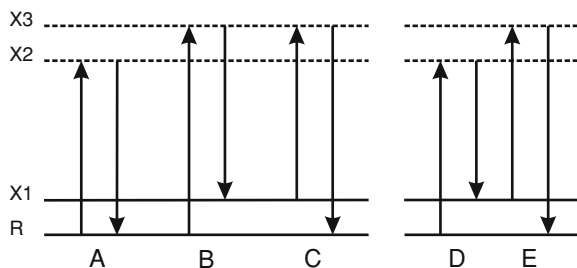


Fig. 4 Energy levels. Incident photons excite molecules to higher virtual energy states. **a** Rayleigh scattering. **b** Stokes scattering. **c** Anti-Stokes scattering. **d, e** Coherent anti-Stokes Raman radiation. **d** Fixed wavelength pump laser excites to X2; the Stokes laser beam facilitates relaxation to X1. **e** The probe laser beam excites molecules at X1–X3, with subsequent relaxation to the ground state. X1 Vibrational energy state. X2, X3 Virtual energy states. R relaxed or ground state

scattering. Similarly, a condition can occur where the molecule is already in a higher virtual energy state when the incoming photon excites the molecule. If the molecule subsequently returns to the relaxed state, the scattered photon will have a higher energy than the incoming photon, resulting in a shorter wavelength. This very rare reaction is called anti-Stokes scattering. Together Stokes and anti-Stokes scattering is called Raman scattering. Raman spectroscopy utilizes a single frequency of radiation for excitation, and the spectrum of frequency shifted emission from the sample is the Raman emission spectrum. The Rayleigh scattering is filtered to leave only the much weaker Raman scattering [126]. Every molecule will result in a characteristic Raman spectrum, which is the result of the combined Raman scattering of the molecular bonds and electron clouds in that particular compound. A complex organism will hence give a complicated spectrum consisting of the overlaid combined spectra from all the molecules (e.g., proteins, fatty acids, nucleic acids, etc.) in the sample, where signature peak heights and positions are representative for individual components of the cells [94]. This can be used to follow the change in chemical composition of single individual cells as a result of, e.g., growth rate or interaction with the environment, and in this way differentiation in a population can be determined on a single-cell level (see examples later in this chapter). Raman spectroscopy can be combined with confocal microscopy to provide 3D information on cell identity or chemical composition of, e.g., extracellular substances (EPS) in biofilms [106, 116, 144].

The Raman scattering is inherently very weak, and a number of methods exist to enhance sensitivity. Surface-enhanced Raman spectroscopy (SERS) is frequently used to amplify the weak Raman signals. In SERS the sample is placed on a typically silver- or gold-covered surface. The physical explanation for the enhancement (up to 10^{11} fold) is not fully elucidated, but it is believed that an increase in the electrical field due to the excitation of the gold or silver surface plasmons by the laser light source boosts the Raman scattering intensity [75]. SERS has successfully been used for identification and characterization of bacteria

[73, 74]. In combination with the AFM, utilizing metal-coated tips, the Raman measuring capability can be combined with very high resolution, enabling chemical mapping of surfaces, e.g., of bacteria down to a molecular scale. In this technique, termed tip-enhanced Raman spectroscopy (TERS), the Raman excitation is performed at the metal-coated AFM tip, linking the atomic force microscopy high-resolution imaging to very localized SERS [20, 98, 100]. Further signal enhancement can be achieved using coherent anti-Stokes Raman spectroscopy (CARS). This technique relies on two laser excitation sources. These two lasers, the fixed frequency pump laser and the tunable Stokes laser, simultaneously excite the molecule to virtual state (X2) and vibrational state (X1) (see Fig. 4d, e): When the Stokes laser has the right frequency, the return from X2 to a lower vibrational energy state (X1) occurs via a stimulated Stokes emission. When the sample molecule is in this state, it can be further excited by a probe laser beam to the higher virtual energy state (X3) (in the actual setup this beam is provided by the Stokes laser). When the molecule relaxes to the ground state (R), it emits a photon with a higher energy than the excitation photon, resulting in an anti-Stokes effect, i.e., a higher frequency [11, 90]. This setup produces coherent anti-Stokes photons resulting in a dramatically enhanced signal. Furthermore, since the emitted Raman scattering has a shorter wavelength than the excitation photons, interference from fluorescence is eliminated [90]. A complication is that so-called phase matching is required to conserve the sum of photon momentum; it means that the strong confined beam of CARS photons is being emitted in its own direction, depending on the direction of the two incoming beams and their frequencies [23]. This method has already been used for imaging of bacterial cells, although at an experimental stage [25, 153]. The emergence of new commercial instruments with CARS-enhanced confocal microscopy gives great promise for the future coupling of structure and chemical composition of microorganisms.

2.9 Presentation and Analysis Software

Many software packages exist for the analysis of microscopy images. They can roughly be divided into: general purpose and dedicated programs, programs for presentation of single images or image stacks, and programs for analytical purposes. Representative examples are provided in Table 1.

3 Bacterial Single-Cell and Biofilm Microscopy, Bistability and Subpopulations

The following sections will concentrate on the phenomenon of bistability in bacterial populations and how microscopy of single cells and biofilm structures has revealed differentiation between cells in a population. *Bacillus subtilis* and

Table 1 Examples of software packages for microscope image processing. Image processing programs

Name	General purpose	Dedicated (instrument specific)	Analytical	2D	3D	Source
ImagePro Plus	X	X ^a	X	X	X	http://www.mediacy.com
ImageJ and NIH Image ^{b, c}	X		X	X	X	[2]
Zeiss ZEN (free viewer available)		X	X ^a	X	X	Carl Zeiss AG, Germany
Leica LAS (free viewer available)		X	X ^a	X	X	Leica Microsystems, Germany
ISA ^d			X	X	X	[87, 149]
ISA3D ^d			X	X	X	[14, 87]
COMSTAT and COMSTAT2 ^b			X		X	[65] http://www.comstat.dk
Daime ^b	X		X	X	X	[34]
Imaris	X	X ^a		(X)	X	http://www.bitplane.ch
Phlip ^b			X	X	X	http://www.phlip.org
MicrAn and ConAn	X		X	X	X	http://www.biocon-online.de

^a Via add-on module
^b Free (public domain)
^c Open source
^d Algorithm source code available

Escherichia coli will be used as the main case studies of bistability, whereas *Pseudomonas aeruginosa* will be used as a model organism in connection to differentiating subpopulations found in biofilms and visualized using confocal microscopy.

3.1 Bistability in *B. subtilis*

3.1.1 Competence

By recent advances in the ability to investigate gene expression on a single-cell level, several studies have demonstrated bistability and differentiation in gene expression. Under certain growth conditions *B. subtilis* cells are able to enter the state of genetic competence, i.e., the bacteria can take up free DNA and incorporate it into their genome by recombination via the process of transformation [38]. When *B. subtilis* enters the stationary phase, competence occurs naturally in a subpopulation of cells and depends this way on the growth phase of the single cell as well as nutrient composition and availability in the near environment [37].

Competence development in *B. subtilis* is regulated by the transcriptional activator ComK, which binds to the *comK* promoter and thus acts as an auto regulator [136]. Fluorescent microscopy of single cells with GFP expression controlled by the *comK* promoter showed that the population divides into two subpopulations when entering the stationary phase, this way demonstrating bistability in competence expression; some cells express *comK* while others do not activate the ComK promoter [92, 127].

When cells are growing exponentially the level of ComK is low as the housekeeping protease complex MecA-ClpC-ClpP is degrading the ComK protein. Furthermore, at least two repressors, Rok and CodY, act on the *comK* promoter. At near stationary phase, quorum sensing results in upregulation of ComS, which will partly block the inactivation of ComK by binding to the MecA-ClpC-ClpP complex [52, 92, 93].

3.1.2 Sporulation

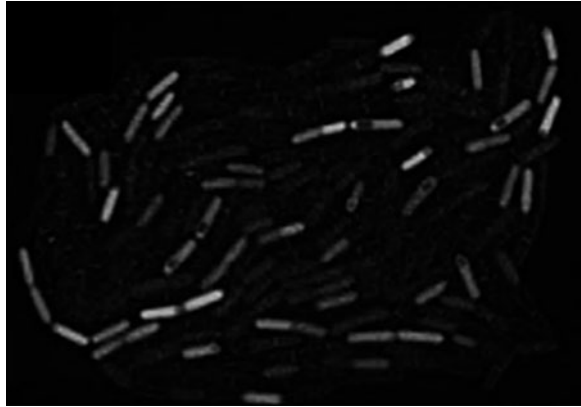
Differentiation in cell types can in some cases be distinguished by cell morphologies using light microscopy, but in many cases a clear picture of different cell types in a population can only be analyzed by use of transcriptional reporter gene fusions for each cell type in combination with fluorescent microscopy, which also will make quantification by flow cytometry of the cell populations possible. Using time-lapse microscopy, it is furthermore possible on a single-cell level to follow dynamic development in growth activity, structure and gene expression using fluorescently labeled appropriate reporter strains. When *B. subtilis* reaches the stationary phase, nutrients become limited, and an endospore will be produced in some, but not all cells. Many cells lyse at this point, liberating nutrients, and the release of the endospore from mother cells eventually takes place. The released nutrients support a second growth period and production of spores. The produced spores will maintain their dormant stage, which is highly resistant to environmental stress until a preferred environmental signal triggers germination.

Like in the case of ComK, the regulatory protein Spo0A has been found to exhibit bistable behavior during sporulation. Using a *gfp* fusion to a promoter under the control of Spo0A, it was shown by fluorescent microscopy that the population revealed a heterogeneous distribution of cells, with only a subpopulation of cells expressing Spo0A [47].

Spo0A is under the control of a positive feedback loop through activation of its own promoter as well as a double repressor system. Spo0A represses *abrB* and AbrB represses *sigH*, an activator of *spo0A*. A high expression of *spo0A* thus is necessary to reduce the AbrB-mediated repression of *sigH* resulting in further expression of *spo0A*. It was demonstrated using CFP and YFP in promoter fusions to AbrB and SpoIIA that expression of the *abrB* and *spoIIA* genes is distinct in individual cells during sporulation, resulting in a bimodal expression profile [140].

Single-cell tracking was used by Veening et al. [139] to investigate three cell forms in *B. subtilis*: spore-forming cells, lysing cells and actively growing cells

Fig. 5 Epigenetic inheritance in a *B. subtilis* sporulation, non-random bistability. The image shows how subfamilies of *spoIIA* Gfp expressing cells (light grey) develop a non-random bistability pattern [141]. Reproduced with permission. Copyright (2008) National Academy of Sciences USA



reappearing after cells had entered stationary phase. It was found that the fate of most cells already is determined before reaching the stationary phase. Cells that result in spore formation will not grow after the exponential phase, whereas cells that start growing actively after the first exponential phase will not become spore formers. A cell population that has lysis as its final cell fate will be able to join both groups of cells. By time-lapse recording of colony development in *B. subtilis*, using a GFP reporter system showing expression of SpoIIA, another regulatory protein regulating spore formation, it was visualized that spore-forming cells in most cases were situated next to each other (light grey cells in Fig. 5). This finding indicated a non-random development of the two subpopulations in a way that cell offspring's will share a phenotype with their parents in a bistable *B. subtilis* population [141].

3.1.3 Motility

Bistability in competence and sporulation in *B. subtilis* is pronounced during the late exponential and stationary growth phase, and fluorescent reporter systems and microscopy have been found useful for demonstrating this phenomenon. A third bistable regulation takes place in *B. subtilis*, namely in cell motility in exponentially growing cells. Only some cells express *sigD*, the sigma factor necessary for flagella production, and the result is a differentiating cell population of motile and non-motile cells. The non-motile cells will often appear as chain-like structures, making it possible to distinguish them from the motile cells even by morphology using light microscopy (Fig. 6) [78].

3.2 Bimodal Gene Expression and Biofilm Formation

For the last decade, it has been well known and accepted that bacteria in most environmental settings live in surface-associated communities called biofilms [28–

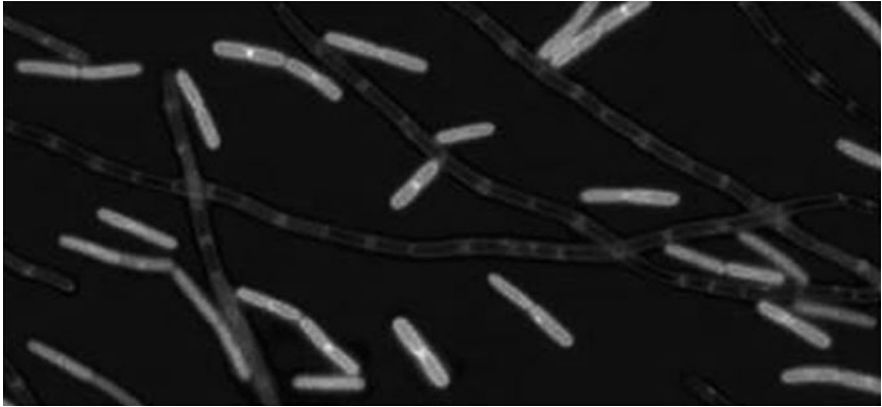


Fig. 6 Differentiation in motility. GFP was fused to the P(*hag*) promoter where *hag* is under control of the alternative sigma factor *sigD*, controlling motility and chaining in *B. subtilis*. Single cells were found GFP positive (light grey), whereas chains of cells did not show GFP expression [78]. Reproduced with permission from Cold Spring Harbor Press

32, 54, 82, 132, 135]. The importance of detailed knowledge about this bacterial lifestyle has proven to be required in order to understand many aspects of bacterial biology and is relevant both in environmental microbiology and medical microbiology. An important part of a biofilm structure in many cases is the presence of an extracellular polymeric substance (EPS) that is produced by the cells and that holds the biofilm structure together. EPS binding material between cells of *E. coli* was demonstrated using atomic force microscopy (Fig. 7) [29, 78].

Vlamakis and colleges [143] have combined gene expression profile studies with spatio-temporal differentiation in matrix-producing, motile and sporulating cells in connection to biofilm development and architecture of *B. subtilis*. In this study fluorescent protein reporter fusions were used to track expression of EPS matrix-producing, sporulating and motile cell types during dynamic biofilm development over a 72-h period. It was found after cell sorting of harvested biofilm cells that motility was upregulated in the initial stages of biofilm formation. That matrix-producing cells started to dominate after 24 h growth, and sporulating cells showed up in the older biofilm after 48 h. All three cell types coexisted in the mature *B. subtilis* biofilm, and production of EPS was carried out by only a subpopulation of cells [24].

Direct localization of the different cell types was also mapped during biofilm growth and maturation, and showed that motile cells dominated in the early biofilm at the top layers and represented only a minor part in the mature biofilm, mainly localized at the substratum. The matrix-producing cells were found randomly throughout the biofilm structure, whereas the sporulating cells were found in the upper structures in the mature biofilm. Using dual reporters it was shown that the mature biofilm harbored all three cell types and that motile cells were

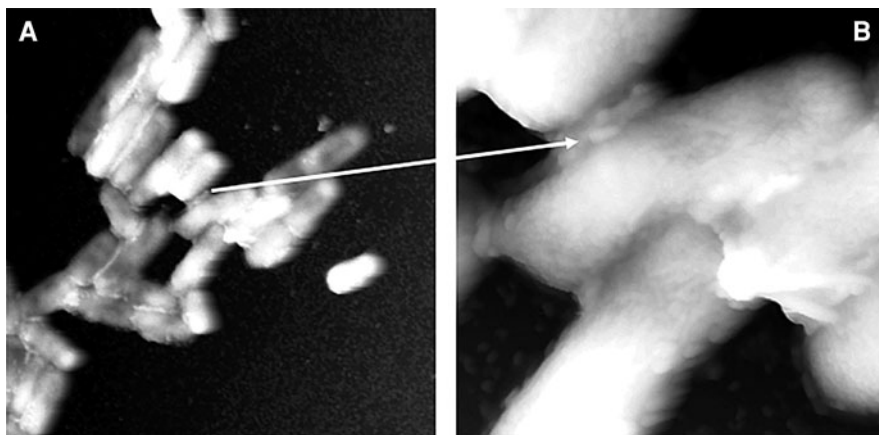


Fig. 7 AFM micrographs showing *E. coli* cells carrying the F plasmid, adhering to each other most likely by their F pili and by virtue of the produced EPS. **a** Cluster of cells and **b** zoomed image of a few cells in **a** showing the binding material between the cells (Haagensen and Sternberg, unpublished)

found mainly in distinct regions relative to sporulating cells that co-existed with the matrix-producing cells (Fig. 8).

Dual fluorescent-reporter systems combined with time-lapse microscopic recording was applied for the investigation of differentiation and transition of the three cell types at a single-cell level. By monitoring CFP-tagged cells reporting motility and YFP-tagged cells reporting matrix production, it was found that motile cells can perform a transition to matrix-producing cells. In the same way, it was shown that matrix-producing cells can turn into sporulating cells, whereas only a few motile cells have the ability to transform into sporulating cells (Fig. 9).

3.3 Persistence and Bistability in *E. coli*

Since the early days of antibiotic treatment of infections, it has been known that some bacteria develop resistance to certain antibiotics. The bacteria can cope with antibiotics by mutation, expressing efflux pumps, releasing indigenous antibiotic inactivation enzymes or the occasional acquisition of resistance-infering genes from the environment. However, a subpopulation of cells in certain bacteria seems to have a different strategy in dealing with environmental stress. They develop persister cells with antibiotic tolerance, which is non-heritable and reversible, meaning that when the antibiotics are not present anymore the cells again become sensitive.

Until recently it has been difficult to isolate and investigate the small amount of persister cells developing in a population. Using microscopy in combination with microfluidic devices, phenotypic switching was studied in *E. coli*. The microfluidic

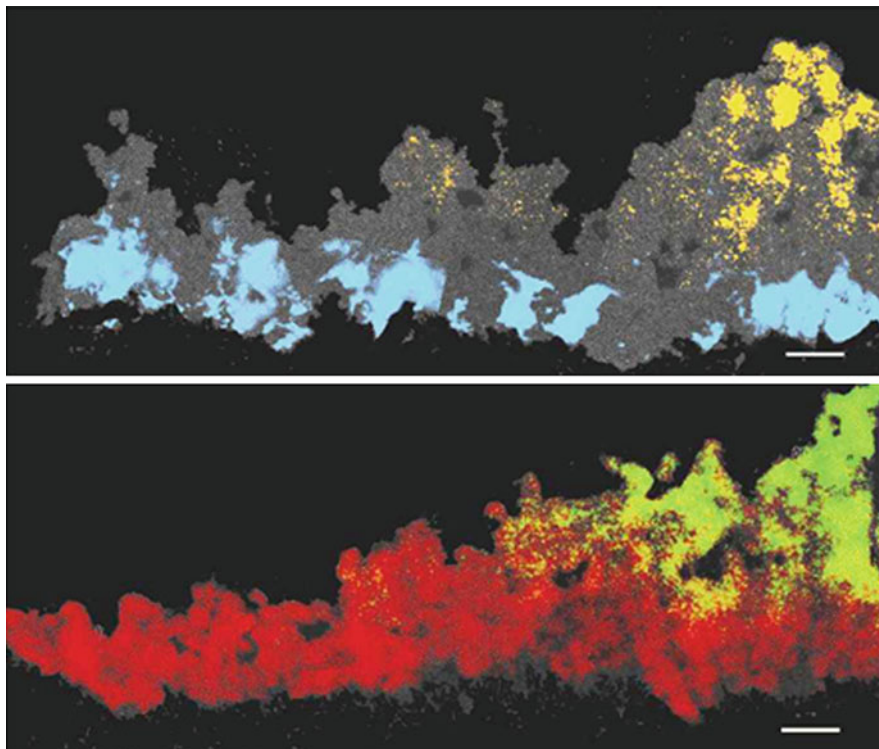


Fig. 8 Micrographs showing biofilm structure of *B. subtilis* and the distribution of motile cells in blue, matrix-producing cells in red and sporulating cells in orange [143]. Reproduced with permission from Cold Spring Harbor Press

channels were dimensioned to only allow propagation in one dimension (Fig. 10) [7]. The system thus allows for monitoring individual cells during growth and response to antibiotics, in this case ampicillin. It was possible to find persister cells already present before antibiotic challenge as a small subpopulation of cells showing a much reduced growth rate. During the antibiotic treatment only the persister cells survived in the microfluidic channels, and after removal of the antibiotic media the persister cells could resume growth (Fig. 10) [7].

Development of persister cells is a spontaneous bet-hedging survival strategy allowing *E. coli* to distribute its population heterogeneously such that some cells at all times are prepared for changing, adverse environmental conditions.

3.4 Raman Microscopy of Bacterial Cells

For *Clostridium* organisms, studies of the cell cycle have shown that cells germinating from spores develop rod-shaped cells, which eventually differentiate into

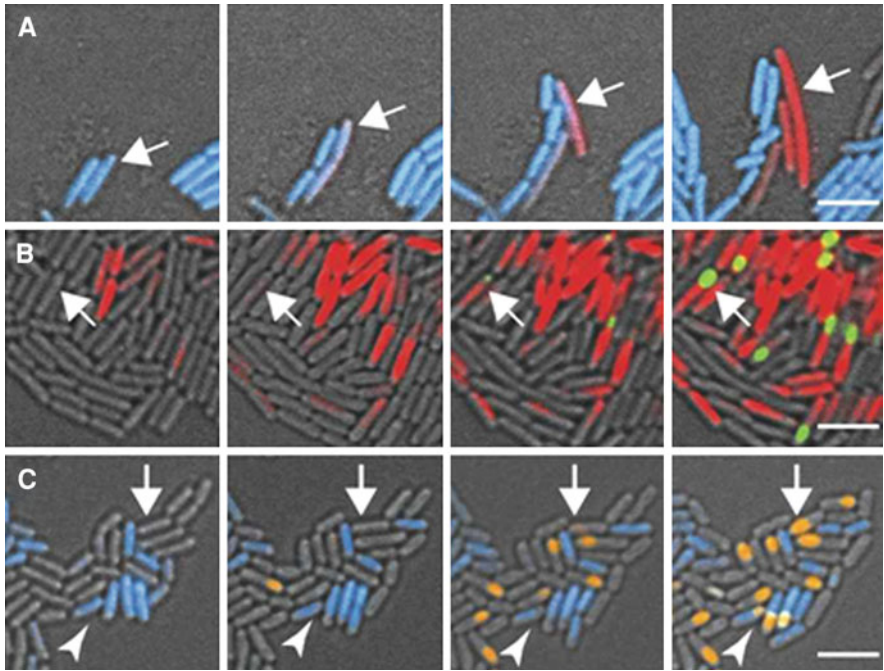


Fig. 9 Micrograph images showing dynamic development of single cells in a biofilm of **a** motile cells in blue and matrix-producing cells in red. The arrow shows a motile cell transitioning to a matrix-producing cell. **b** Matrix-producing cells in red and sporulating cells in green. The arrow shows matrix development followed by transitioning to a sporulation cell. **c** Motile cells in blue and sporulating cells in orange. The arrow shows that sporulating cells arise from non-motile cells (a few sporulating cells arise from motile cells, arrowhead) [143]. Reproduced with permission from Cold Spring Harbor Press

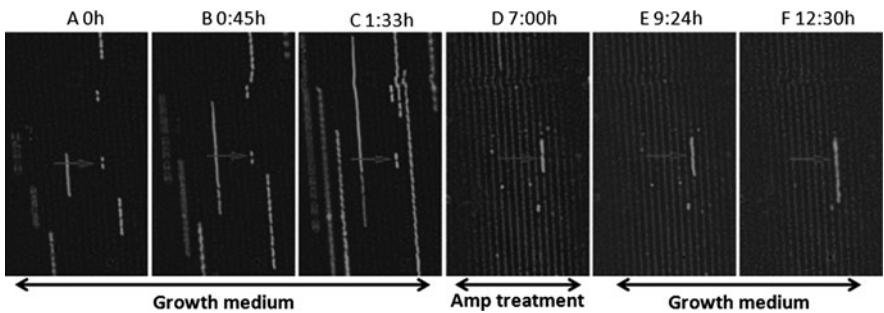


Fig. 10 Micrographs showing *E. coli* cells growing in a microfluidic chamber. Only slow-growing persister cells survived antibiotic treatment. **a–c** Cells are dividing and growing in narrow channels allowing the growth rate of the single cells to be monitored as the length of strings of cells developing over time. **d** Cells were exposed to ampicillin for 4 h. **e, f** After washing, cells were changed back to growth medium without ampicillin [7]. Reprinted with permission from AAAS

clostridial cell forms after which spores start to become visible. In this study it was demonstrated that Raman microscopy enables investigations of differentiation in cell physiology and composition on a single-cell level during the cell cycle of *C. acetobutylicum* [119]. In other examples, Raman microscopy has shown potential for investigation of the consequences of antibiotic treatment of bacterial cells [58, 99] and to differentiate between planktonic and biofilm-associated *Pseudomonas putida* cells [70]. Raman spectroscopy also has been used as a tool to determine identity of bacterial cells, although this requires a large training set (database) of spectra from already identified bacteria of the type to be determined, which by itself is not a trivial task [58, 113], reviewed recently by Harz [59].

3.5 *Pseudomonas aeruginosa* Biofilm Development and Differentiating Subpopulations

Pseudomonas aeruginosa has been used extensively for the study of microbial biofilm formation, and many of the most important contributions to our understanding of biofilm development comes from these studies. Lately, this organism has also been subject to differentiation studies and clinically relevant antibiotic treatment studies with the goal to investigate phenotypic heterogeneity in biofilm populations [9, 72, 80, 102, 148]. A combination of fluorescent reporter strains, confocal microscopy, fluorescent recovery after photo-bleaching (FRAP) and real-time microscopy has made it possible to follow the spatial distribution of phenotypic subpopulation development.

A mature biofilm of *P. aeruginosa* can be described as a mushroom-shaped structure composed of two major subpopulations, a subpopulation situated close to the substratum and a subpopulation forming the top of the mushroom [80]. The diversification into two subpopulations was shown by combining growth of GFP tagged *P. aeruginosa* in flow chambers with confocal time lapse microscopy in combination with FRAP. The GFP signal from cells in a section of a mature microcolony was bleached using high-intensity laser illumination in a rectangular region along the biofilm structure. The bleached area was monitored at small time intervals with respect to GFP fluorescent single-cell appearance. It was demonstrated that two populations of *P. aeruginosa* exist, one motile subpopulation forming the outer layer of the structure and able to move into the bleached region and one non-motile population forming the core of the microcolony (Fig. 11a–c) [72]. Furthermore, the phenotypic diversity and two-population development were demonstrated using a 1:1 mixture of a wild-type *P. aeruginosa* tagged with YFP and a non-motile *pilA* mutant of *P. aeruginosa* tagged with CFP. The role of the two populations in forming the final biofilm structure was in this way shown on a single-cell level as well as on a 3D structural level (Fig. 11d, e) [80, 103]. Interestingly, it was found that upon antimicrobial treatment of this biofilm, only one of the two subpopulations was sensitive to compounds like colistin,

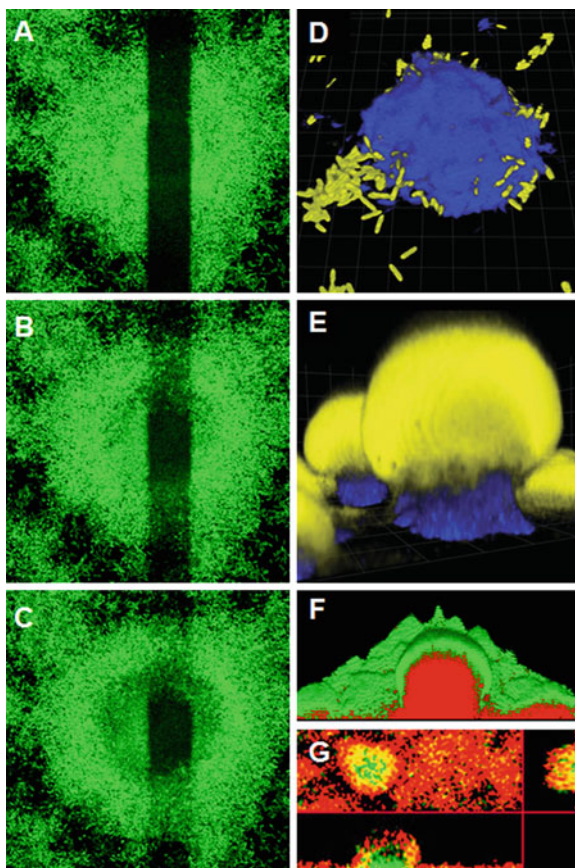


Fig. 11 Micrographs showing a *top-down* view of GFP-tagged PAO1 cells in a microcolony. FRAP was applied to the colony by bleaching a rectangular area across the colony (**a**), followed by time-lapse recording using confocal laser scanning microscopy of the cells. **b** and **c** Show how only cells located in the periphery of the microcolony are motile and cover the bleached area [72]. **d** and **e** The initial development and the final mature 3D structure respectively of a mixture of motile PAO1 tagged with YFP (yellow) and a PAO1 pilA mutant tagged with CFP (blue) [103]. Reproduced with permission from John Wiley & Sons. Micrographs **f**, **g** shows 3D structure representations of live (GFP-tagged green cells) and dead [propidium iodide (PI)-stained red cells] distributed after treatment with colistin and ciprofloxacin, respectively [72, 102 and Haagensen, unpublished]

tetracycline, ciprofloxacin, etc., implying that *P. aeruginosa* forms different subpopulations to have a higher chance of handling incoming perturbations. The surviving subpopulation of cells exhibits phenotypic tolerance and not resistance, as surviving biofilm cells harvested from antimicrobial-treated biofilms exhibit the same antimicrobial susceptibility phenotype as the cells that were used to initiate the biofilm (Fig. 11f, g) [72, 102].

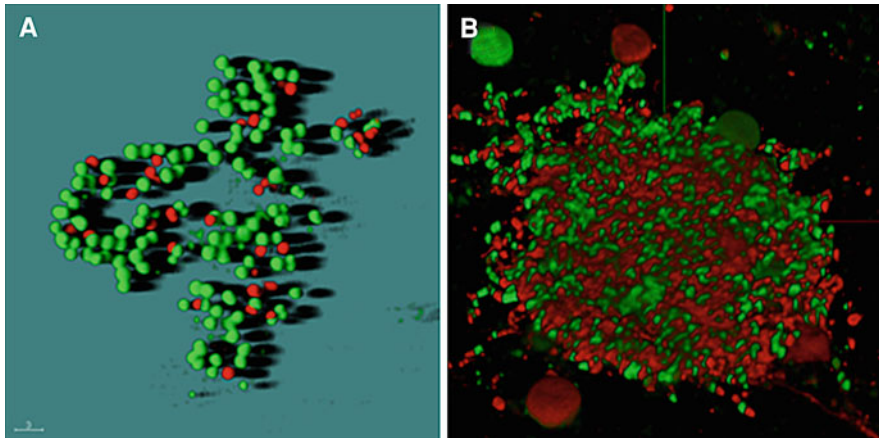


Fig. 12 Micrograph shows 3D structure representations of live (Syto9-stained *green* cells) and dead (PI-stained *red* cells) cells from cystic fibrosis patients undergoing intensive antibiotic treatment. Cells were stained immediately after sampling (Haagenzen unpublished)

In sputum obtained from cystic fibrosis patients undergoing intensive antibiotic treatment, LIVE/DEAD[®] staining (Invitrogen, CA) in combination with confocal microscopy indicated that potentially persistent cells appear frequently. Colistin, a membrane-targeting agent, was used during the treatment, and cell sorting followed by plating of live and dead cells confirmed the existence of two populations and persistence of cells also upon antibiotic used in treatment (Fig. 12). As described for *E. coli*, growth rate-dependent development of tolerant cells and phenotypic differentiation are important survival strategies also for *P. aeruginosa*.

4 Yeast Single-cell and Biofilm Microscopy

Historically, microscopy of yeast cells has focused on free-living cells in pure culture. In this respect the yeast *Saccharomyces cerevisiae* has served as a successful model for the study of organelles and cell structures in the eukaryotic cell. *S. cerevisiae* is easily genetically modified, has a fast reproduction time and perhaps most importantly a large number of community resources exists, such as a complete set of GFP-tagged proteins and targeted knockout mutants of all genes in the genome [45, 71]. Though relatively small in comparison to other eukaryotic cells, with a cell size of 3–5 μm , *S. cerevisiae* live cell imaging has excelled in recent years with the development of STED microscopy and beam-scanning multifocal multiphoton confocal microscopy, which have led to resolution limits much below 100 nm [41, 79] (and Stelzer, this volume).

4.1 Cell-to-Cell Variation in Yeast Populations

As with bacteria, biochemical assays for yeast cells are based on the assumption that protein expression and localization are uniform throughout a population of isogenic cells. Genetic tools however are widely used to investigate cell-to-cell variation within a population. Examples of these are mating type switching in haploid cells, mating between cells of different mating type [129], a morphological shift in *S. cerevisiae* from a yeast to a pseudohyphal form and a shift in *Candida albicans* from a yeast to a filamentous phenotype [46, 88]. More recently, microscopic methods have been applied to screen for cell-to-cell variation in gene expression within populations.

GFP tagging of 4,156 *S. cerevisiae* proteins in individual cell lines has been used to identify and verify protein localization by fluorescence microscopy [71]. While many proteins have specific cellular localization, some proteins vary their localization between cells. A classical example of this is the uneven distribution of the *S. cerevisiae* mating type switching protein (Ash1p) between mother and daughter cells. Ash1p is asymmetrically distributed in a way that the concentration of Ash1p is higher in the daughter nucleus where it inhibits mating type switching [124]. Ash1p asymmetry is regulated at the mRNA level, with mRNA synthesized in the mother cells being transported to the daughter cell. This was elegantly shown in living yeast cells by fluorescence microscopy of *ASH1* mRNAs interacting with a GFP-labeled MS2 bacteriophage coat protein through a stem loop structure introduced into the mRNA [12]. Tagging of mRNA with GFP-MS2 was later used to show that most mRNA species in *S. cerevisiae* have a specific location in the cell and that localization is uniform among cells in a population [53, 151].

Protein abundance seems to vary much within populations. To understand the background of variation, Weissman and coworkers measured the abundance of 2500 protein in individual clones at the single-cell level [101]. They performed high-throughput flow cytometry of a library of GFP-tagged yeast strains and discovered that variation in protein expression is largely caused by stochastic variation at the level of mRNA. Interestingly, there are drastic differences in noise between the functional classes of proteins in *S. cerevisiae*. Genes responding to environmental changes encode gene products with large variation, while proteins involved in structural processes vary less. These differences may reflect selective pressure for a given level of variation, where cellular processes that require accuracy will select for low variation. Large variation, however, may permit a population to express multiple phenotypes to optimize average fitness in changing environments.

4.2 Bistability in Yeasts

Subpopulations with inheritable differential expression of certain genes due to bistability are known from the common human opportunistic pathogenic yeast *C.*

albicans. *C. albicans* can switch between spherical cells that form white colonies and bigger elongated cells that form opaque colonies [110, 125]. Bistability is regulated at the genetic level by the transcription factor Wor1p that is present in very low amounts in white cells and accumulates in opaque cells. Wor1p binds to the promoter of its own gene and induces its expression in a positive feedback loop [69, 152]. The positive feedback loop in combination with stochastic variation in Wor1p expression is suggested to be responsible for switching and inheritance of white and opaque states.

While investigations of bistability in *C. albicans* have been driven by macroscopic features, advanced microscopy such as microscopic high-content screening and high throughput flow cytometry combined with libraries of strains with GFP-tagged proteins may likely lead to the discovery of bistability in *S. cerevisiae* [33, 71, 101, 142].

4.3 Microscopy of *Candida albicans* Biofilm

Microscopy of yeast communities has become increasingly important with a growing number of human infections caused by fungal biofilm on catheters and implants (recently reviewed by Ramage [108]). Biofilms from the most common fungal pathogens, *Candida* spp., are currently being studied by scanning electron microscopy and confocal laser scanning microscopy (CLSM). While scanning electron microscopy reveals biofilm organization and extracellular matrix [26], CLSM can be used to monitor live cell biofilm development in three dimensions over time [26, 108, 120]. Recently atomic force microscopy has also been used to visualize the surface structure of the *C. albicans* biofilm, though the full potential of the AFM for this purpose has probably not been fully exploited yet [84].

A mature biofilm of *C. albicans* is composed of two morphotypes, a unicellular yeast and a multicellular hyphal form [6, 26]. Scanning electron microscopy revealed that both morphotypes can form biofilm individually, though the coexistence of hyphae with yeast cells appears to be essential for a dense biofilm [6]. Deletion of genes essential for filamentous growth in *C. albicans* leads to thin biofilms composed solely of unicellular yeast cells. Biofilms composed of hyphae are dense and appear to lack channel-like structures found in the wild-type *C. albicans* biofilms.

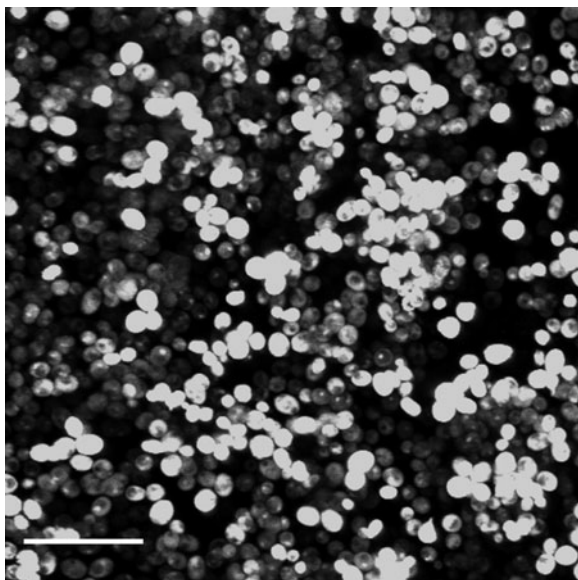
While morphology of *C. albicans* biofilms is well understood, little is known about the molecular mechanism underlying biofilm formation [108]. A limiting factor in this respect is the choice of model organism. Genetic modifications and screens in *Candida* species are cumbersome and often hampered by the existence of paralogous genes that mask the phenotype of a gene deletion. The closely related yeast, *S. cerevisiae*, offers an attractive alternative with its ability to form biofilm [109] and the ease by which genetic modifications can be carried out in this organism. To further develop *S. cerevisiae* as a model for biofilm studies, we have recently developed CLSM methods for the study of biofilms of this organism.

4.4 Confocal Microscopy of *S. cerevisiae* Biofilms on Batch Culture Slides and in Flow Chambers

Saccharomyces cerevisiae biofilm formation and development can be studied by CLSM (Fig. 13) applying the batch culture slide method described for *C. albicans* and *C. glabrata* with the modifications described in the figure legends to Fig. 13 [120].

With few exceptions, *S. cerevisiae* biofilms can be studied in flow cells according to the protocol applied for *P. aeruginosa* (Fig. 14; [131]). A necessary development was the choice of surface where *S. cerevisiae* can adhere and form biofilm. While *P. aeruginosa* and many other bacteria readily attach to silica surfaces, *S. cerevisiae* adheres poorly to glass surfaces. Suitable surfaces for *S. cerevisiae* biofilm formation are plastics such as, e.g., polyethylene (PE), polypropylene (PP) and to a lesser extent polyvinylchloride (PVC), which were first described for *S. cerevisiae* biofilm assays [109]. Besides these polymers, different polyesters and slides coated with collagen or poly-L-lysine are suitable substrates for *S. cerevisiae* biofilm assays in batch as well as flow cells (unpublished). While plastic cover slides are applicable as biofilm surfaces, several of them suffer from autofluorescence that disturbs CLSM visualization. Coverslips such as the Thermanox PE are autofluorescent in the range 380–545 nm, excluding work with blue and green dyes such as the vital stain Syto9 (Invitrogen, Irvine, CA), GFP and CFP. PVC on the other hand is without autofluorescence in the visible range and therefore an optimal choice as a surface for yeast biofilm imaging (Fig. 15).

Fig. 13 CLSM of *S. cerevisiae* (CEN.PK113.7D *sfl1*) batch biofilm after 24-h growth in synthetic complete medium with amino acids and 2% glucose (SC-ura). Cells were grown in a Lab-TekTM Chamber SlideTM System; Permanox[®] (NUNC, Denmark) in 1 ml medium and stained 30 min with Syto9. Bottom left bar 30 μ m. CLSM was performed with a Zeiss LSM510 microscope using a 63x/0.95NA water immersion lens. Bar 30 μ m



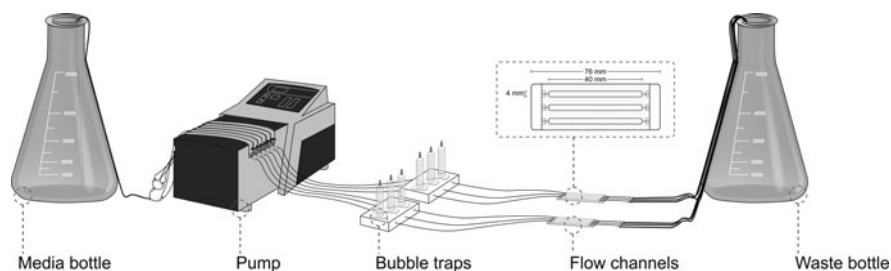


Fig. 14 Experimental setup for *S. cerevisiae* biofilm in flow cells. A flow cell with flow channels is covered with a PVC cover slip that serves as a surface for yeast biofilm attachment and development. A peristaltic pump ensures constant flow of media from the media bottle through the flow channels

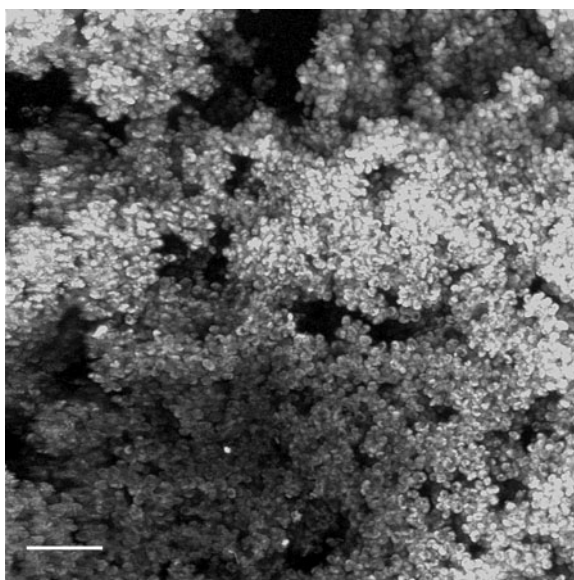


Fig. 15 CLSM of *S. cerevisiae* (CEN.PK113.7D *sfl1*) biofilm in the flow cell setup shown in Fig. 14. Image was recorded after 42 h growth in continuous flow of synthetic complete medium with amino acids and 0.02% glucose (SC-ura). Biofilm formed on PVC cover slips (Rinzl, Electron Microscopy Sciences, Hatfield, PA) and was visualized by staining with Syto9. CLSM was performed with a Zeiss LSM510 microscope using a 40x/1.3NA oil immersion lens. Bar 30 μ m

Secondly, *S. cerevisiae* biofilm formation is dependent on a haploid cell state [109] and expression of cell surface adhesins such as Flo11p (Muc1p) or Flo1p. Most laboratory strains as well as many natural isolates of *S. cerevisiae* do not express the *FLO11* gene or other adhesion genes [43], and they are therefore not directly applicable for biofilm studies. The *S. cerevisiae* strain background of choice for biofilm studies has so far been strain Σ 1278b [109]. However, mutants

of other strain backgrounds such as S288c or CEN.PK may be used to study biofilms of *S. cerevisiae* if these strains express the *FLO1* or *FLO11* genes [43].

Besides the use of *S. cerevisiae* for identification of genes involved in yeast biofilm formation, maturation and detachment, *S. cerevisiae* biofilm in both batch and flow cells can effectively be screened for susceptibility to fungicides. Molecular targets for fungicides as well as fungicide resistance mechanisms may be uncovered by the combination of barcode-target yeast mutants and fluorescence microscopic high-content screening.

5 Future Perspectives

While the novel advances in microscopy have proven useful for investigation of microbial communities and microbial single cells, biological discoveries made on the basis of these technologies are only starting to emerge.

One major opportunity is to resolve live objects below the theoretical optical resolution of 200–250 nm with methods such as STED, STORM and SIM. These improved resolution limits enable increased insight into complex spatiotemporal processes such as cell cycle, DNA repair and DNA organization. Higher resolution of fluorescent tagged proteins and RNAs of unknown function that co-localize with others of known function will further aid in the assignment of function to the large group of genes with hitherto unknown role in the cell. Combined with Raman spectroscopy, high-resolution microscopy can also provide information on the molecular basis, localization and structure of extracellular matrix that is otherwise difficult to obtain.

Nanoscale spatial resolution by AFM facilitates visualization of cell surface structures such as extracellular polymers, flagella and pili. At the macromolecular level, the AFM has already proven to provide novel understanding of interactions between macromolecules, e.g., for protein-DNA binding kinetics.

Another aspect of the new technologies is high content automated screening. Automated high-resolution microscopy combined with libraries of, e.g., GFP-tagged proteins or knock-out mutants allows integrated analysis of antibiotic resistance, signal transduction, expression patterns and many other aspects of cell biology and physiology. As mentioned previously, screening of expression patterns is likely to reveal novel examples of bistabilities in microorganisms that are not readily recognized at the macroscopic level. High content automated screening may also find its application in evolution biology where clones of populations that have undergone experimental evolution may be screened for phenotypic differentiation.

Finally, physiological measurements of microbial cells in complex communities, with methods such as confocal Raman microscopy, will provide valuable insight into the physiology of complex microbial communities with respect to cross feeding between species and cell types, local gradients and organization of communities, and internal changes in metabolism. Information about physiological

processes in complex microbial communities has a high impact on our basic understanding of microorganisms and applied applications in biotechnology.

Acknowledgments This work was supported by grants from the Carlsberg Foundation and the Lundbeck Foundation to Janus A. J. Haagenzen. Birgitte Regenberg was supported by The Danish Council for Independent Research | Natural Sciences (FNU). Claus Sternberg was supported by a grant from the Danish National Advanced Technology Foundation. The authors wish to thank Dr. Ninell P. Mortensen for information about atomic force microscopy, Dr. Rolf W. Berg for information about coherent anti-Stokes Raman spectroscopy and Rune L. Jensen for Fig. 14.

References

1. Abbe E (1873) Beiträge zur Theorie des Mikroskops und der mikroskopischen Wahrnehmung. Arch Mikrosk Anat 9:413–468
2. Abramoff MD, Magalhães PJ, Ram SJ (2004) Image processing with ImageJ. Biophotonics Int 11:36–41
3. Alfano RR, Shapiro SL (1970) Direct distortion of electronic clouds of rare-gas atoms in intense electric fields. Phys Rev Lett 24:1217
4. Alfano RR, Shapiro SL (1970) Observation of self-phase modulation and small-scale filaments in crystals and glasses. Phys Rev Lett 24:592
5. Amro NA, Kotra LP, Wadu-Mesthrige K et al (2000) High-resolution atomic force microscopy studies of the *Escherichia coli* outer membrane: structural basis for permeability. Langmuir 16:2789–2796
6. Baillie GS, Douglas LJ (1999) Role of dimorphism in the development of *Candida albicans* biofilms. J Med Microbiol 48:671–679
7. Balaban NQ, Merrin J, Chait R et al (2004) Bacterial persistence as a phenotypic switch. Science 305:1622–1625
8. Ball CS (1966) The early history of the compound microscope. Bios 37:51–60
9. Barken KB, Pamp SJ, Yang L et al (2008) Roles of type IV pili, flagellum-mediated motility and extracellular DNA in the formation of mature multicellular structures in *Pseudomonas aeruginosa* biofilms. Environ Microbiol 10:2331–2343
10. Bates M, Huang B, Dempsey GT et al (2007) Multicolor super-resolution imaging with photo-switchable fluorescent probes. Science 317:1749–1753
11. Begley RF, Harvey AB, Byer RL (1974) Coherent anti-Stokes Raman spectroscopy. Appl Phys Lett 25:387–390
12. Bertrand E, Chartrand P, Schaefer M et al (1998) Localization of ASH1 mRNA particles in living yeast. Mol Cell 2:437–445
13. Betzig E, Patterson GH, Sougrat R et al (2006) Imaging intracellular fluorescent proteins at nanometer resolution. Science 313:1642–1645
14. Beyenal H, Donovan C, Lewandowski Z et al (2004) Three-dimensional biofilm structure quantification. J Microbiol Methods 59:395–413
15. Binnig G, Quate CF, Gerber C (1986) Atomic force microscope. Phys Rev Lett 56:930
16. Birk H, Engelhardt J, Storz R et al (2002) Programmable beam-splitter for confocal laser scanning microscopy. In: Three-dimensional and multidimensional microscopy: image acquisition and processing, vol IX. SPIE, San Jose
17. Bolshakova AV, Kiselyova OI, Filonov AS et al (2001) Comparative studies of bacteria with an atomic force microscopy operating in different modes. Ultramicroscopy 86:121–128
18. Borlinghaus R, Gugel H, Albertano P et al (2006) Closing the spectral gap: the transition from fixed-parameter fluorescence to tunable devices in confocal microscopy. In: Three-

- dimensional and multidimensional microscopy: image acquisition and processing, vol XIII. SPIE, San Jose
19. Braga PC, Ricci D (1998) Atomic force microscopy: application to investigation of *Escherichia coli* morphology before and after exposure to cefodizime. *Antimicrob Agents Chemother* 42:18–22
 20. Budich C, Neugebauer U, Popp J et al (2008) Cell wall investigations utilizing tip-enhanced Raman scattering. *J Microsc* 229:533–539
 21. Caldwell DE, Korber DR, Lawrence JR (1992) Imaging of bacterial cells by fluorescence exclusion using scanning confocal laser microscopy. *J Microbiol Methods* 15:249–261
 22. Camesano TA, Natan MJ, Logan BE (2000) Observation of changes in bacterial cell morphology using tapping mode atomic force microscopy. *Langmuir* 16:4563–4572
 23. Carreira LA, Goss LP, Malloy TB Jr (1981) Applications of CARS to condensed phase systems. In: Harvey AB (ed) *Chemical applications of nonlinear Raman spectroscopy*. Academic Press, New York
 24. Chai Y, Chu F, Kolter R et al (2008) Bistability and biofilm formation in *Bacillus subtilis*. *Mol Microbiol* 67:254–263
 25. Chan JW, Winhold H, Lane SM et al (2005) Optical trapping and coherent anti-Stokes Raman scattering (CARS) spectroscopy of submicron-size particles. *Sel Top Quantum Electron J IEEE* 11:858–863
 26. Chandra J, Kuhn DM, Mukherjee PK et al (2001) Biofilm formation by the fungal pathogen *Candida albicans*: development, architecture, and drug resistance. *J Bacteriol* 183: 5385–5394
 27. Chatterjee A, Kaznessis YN, Hu WS (2008) Tweaking biological switches through a better understanding of bistability behavior. *Curr Opin Biotechnol* 19:475–481
 28. Christensen BB, Sternberg C, Andersen JB et al (1999) Molecular tools for study of biofilm physiology. *Methods Enzymol* 310:20–42
 29. Costerton JW, Lewandowski Z, DeBeer D et al (1994) Biofilms, the customized microniche. *J Bacteriol* 176:2137–2142
 30. Costerton JW (1995) Overview of microbial biofilms. *J Ind Microbiol* 15:137–140
 31. Costerton JW, Lewandowski Z, Caldwell DE et al (1995) Microbial biofilms. *Annu Rev Microbiol* 49:711–745
 32. Costerton JW (1999) Introduction to biofilm. *Int J Antimicrob Agents* 11:217–221
 33. Czechowska K, Johnson DR, van dM Jr (2008) Use of flow cytometric methods for single-cell analysis in environmental microbiology. *Curr Opin Microbiol* 11:205–212
 34. Daims H, Lucker S, Wagner M (2006) daime, a novel image analysis program for microbial ecology and biofilm research. *Environ Microbiol* 8:200–213
 35. Davidson CJ, Surette MG (2008) Individuality in bacteria. *Annu Rev Genet* 42:253–268
 36. Denk W, Strickler JH, Webb WW (1990) Two-photon laser scanning fluorescence microscopy. *Science* 248:73–76
 37. Dubnau D (1991) The regulation of genetic competence in *Bacillus subtilis*. *Mol Microbiol* 5:11–18
 38. Dubnau D (1991) Genetic competence in *Bacillus subtilis*. *Microbiol Rev* 55:395–424
 39. Dubnau D, Losick R (2006) Bistability in bacteria. *Mol Microbiol* 61:564–572
 40. Dyba M, Keller J, Hell SW (2005) Phase filter enhanced STED-4pi fluorescence microscopy: theory and experiment. *New J Phys* 134:1–21
 41. Egner A, Jakobs S, Hell SW (2002) Fast 100-nm resolution three-dimensional microscope reveals structural plasticity of mitochondria in live yeast. *Proc Natl Acad Sci USA* 99:3370–3375
 42. Eklund H, Roos A, Eng ST (1975) Rotation of laser beam polarization in acousto-optic devices. *Opt Quant Electron* 7:73–79
 43. Fichtner L, Schulze F, Braus GH (2007) Differential Flo8p-dependent regulation of FLO1 and FLO11 for cell-cell and cell-substrate adherence of *S. cerevisiae* S288c. *Mol Microbiol* 66:1276–1289

44. Gad M, Ikai A (1995) Method for immobilizing microbial cells on gel surface for dynamic AFM studies. *Biophys J* 69:2226–2233
45. Giaever G, Chu AM, Ni L et al (2002) Functional profiling of the *Saccharomyces cerevisiae* genome. *Nature* 418:387–391
46. Gimeno CJ, Ljungdahl PO, Styles CA et al (1992) Unipolar cell divisions in the yeast *Saccharomyces-Cerevisiae* lead to filamentous growth—regulation by starvation and Ras. *Cell* 68:1077–1090
47. Gonzalez-Pastor JE, Hobbs EC, Losick R (2003) Cannibalism by sporulating bacteria. *Science* 301:510–513
48. Gustafsson MGL (2000) Surpassing the lateral resolution limit by a factor of two using structured illumination microscopy. *J Microsc* 198:82–87
49. Gustafsson MGL (2005) Nonlinear structured-illumination microscopy: wide-field fluorescence imaging with theoretically unlimited resolution. *Proc Natl Acad Sci USA* 102:13081–13086
50. Guthold M, Bezanilla M, Erie DA et al (1994) Following the assembly of RNA polymerase–DNA complexes in aqueous solutions with the scanning force microscope. *Proc Natl Acad Sci USA* 91:12927–12931
51. Göppert-Mayer M (1931) Über Elementarakte mit zwei Quantensprüngen. *Ann Phys* 401:273–294
52. Hahn J, Kong L, Dubnau D (1994) The regulation of competence transcription factor synthesis constitutes a critical control point in the regulation of competence in *Bacillus subtilis*. *J Bacteriol* 176:5753–5761
53. Haim L, Zipor G, Aronov S et al (2007) A genomic integration method to visualize localization of endogenous mRNAs in living yeast. *Nat Methods* 4:409–412
54. Hall-Stoodley L, Costerton JW, Stoodley P (2004) Bacterial biofilms: from the natural environment to infectious diseases. *Nat Rev Microbiol* 2:95–108
55. Hallett P, Offer G, Miles MJ (1995) Atomic-force microscopy of the myosin molecule. *Biophys J* 68:1604–1606
56. Hansma HG, Vesenka J, Siegerist C et al (1992) Reproducible imaging and dissection of plasmid DNA under liquid with the atomic force microscope. *Science* 256:1180–1184
57. Harke B, Keller J, Ullal CK et al (2008) Resolution scaling in STED microscopy. *Opt Express* 16:4154–4162
58. Harz M, Rösch P, Peschke KD et al (2005) Micro-Raman spectroscopic identification of bacterial cells of the genus *Staphylococcus* and dependence on their cultivation conditions. *Analyst* 130:1543–1550
59. Harz M, Rösch P, Popp J (2009) Vibrational spectroscopy—a powerful tool for the rapid identification of microbial cells at the single-cell level. *Cytometry Part A* 75A:104–113
60. Heimstädt O (1911) Das Fluoreszenzmikroskop. *Z Wiss Mikrosk* 28:330–337
61. Hein B, Willig KI, Hell SW (2008) Stimulated emission depletion (STED) nanoscopy of a fluorescent protein-labeled organelle inside a living cell. *Proc Natl Acad Sci USA* 105:14271–14276
62. Heintzmann R, Jovin TM, Cremer C (2002) Saturated patterned excitation microscopy? A concept for optical resolution improvement. *J Opt Soc Am A* 19:1599–1609
63. Hell SW (2003) Toward fluorescence nanoscopy. *Nat Biotechnol* 21:1347–1355
64. Hess ST, Girirajan TPK, Mason MD (2006) Ultra-high resolution imaging by fluorescence photoactivation localization microscopy. *Biophys J* 91:4258–4272
65. Heydorn A, Nielsen AT, Hentzer M et al (2000) Quantification of biofilm structures by the novel computer program COMSTAT. *Microbiol* 146(10):2395–2407
66. Hirvonen L, Wicker K, Mandula O et al (2009) Structured illumination microscopy of a living cell. *Eur Biophys J* 38:807–812
67. Hopt A, Neher E (2001) Highly nonlinear photodamage in two-photon fluorescence microscopy. *Biophys J* 80:2029–2036
68. Huang B, Wang W, Bates M et al (2008) Three-dimensional super-resolution imaging by stochastic optical reconstruction microscopy. *Science* 319:810–813

69. Huang G, Wang H, Chou S et al (2006) Bistable expression of WOR1, a master regulator of white-opaque switching in *Candida albicans*. *Proc Natl Acad Sci USA* 103:12813–12818
70. Huang W, Ude S, Spiers A (2007) *Pseudomonas fluorescens* SBW25 biofilm and planktonic cells have differentiable Raman spectral profiles. *Microb Ecol* 53:471–474
71. Huh WK, Falvo JV, Gerke LC et al (2003) Global analysis of protein localization in budding yeast. *Nature* 425:686–691
72. Haagenen JA, Klausen M, Ernst RK et al (2007) Differentiation and distribution of colistin- and sodium dodecyl sulfate-tolerant cells in *Pseudomonas aeruginosa* biofilms. *J Bacteriol* 189:28–37
73. Jarvis RM, Brooker A, Goodacre R (2006) Surface-enhanced Raman scattering for the rapid discrimination of bacteria. *Faraday Discuss* 132:281–292
74. Jarvis RM, Goodacre R (2008) Characterisation and identification of bacteria using SERS. *Chem Soc Rev* 37:931–936
75. Jeanmaire DL, Van Duyne RP (1977) Surface Raman spectroelectrochemistry: Part I. Heterocyclic, aromatic, and aliphatic amines adsorbed on the anodized silver electrode. *J Electroanal Chem* 84:1–20
76. Juette MF, Gould TJ, Lessard MD et al (2008) Three-dimensional sub-100 nm resolution fluorescence microscopy of thick samples. *Nat Methods* 5:527–529
77. Kasas S, Ikai A (1995) A method for anchoring round shaped cells for atomic force microscope imaging. *Biophys J* 68:1678–1680
78. Kearns DB, Losick R (2005) Cell population heterogeneity during growth of *Bacillus subtilis*. *Genes Dev* 19:3083–3094
79. Klar TA, Jakobs S, Dyba M et al (2000) Fluorescence microscopy with diffraction resolution barrier broken by stimulated emission. *Proc Natl Acad Sci USA* 97:8206–8210
80. Klausen M, Aaes-Jorgensen A, Molin S et al (2003) Involvement of bacterial migration in the development of complex multicellular structures in *Pseudomonas aeruginosa* biofilms. *Mol Microbiol* 50:61–68
81. Knight JC, Birks TA, Russell PSJ et al (1996) All-silica single-mode optical fiber with photonic crystal cladding. *Opt Lett* 21:1547–1549
82. Kolter R, Greenberg EP (2006) Microbial sciences: the superficial life of microbes. *Nature* 441:300–302
83. König K (2000) Multiphoton microscopy in life sciences. *J Microsc* 200:83–104
84. Lal P, Sharma D, Pruthi P et al (2009) Exopolysaccharide analysis of biofilm-forming *Candida albicans*. *J Appl Microbiol* 109:128–136
85. Lawrence JR, Korber DR, Hoyle BD et al (1991) Optical sectioning of microbial biofilms. *J Bacteriol* 173:6558–6567
86. Le CE, Frechon D, Barry M et al (1994) Observation of binding and polymerization of Fur repressor onto operator-containing DNA with electron and atomic force microscopes. *Proc Natl Acad Sci USA* 91:11816–11820
87. Lewandowski Z, Beyenal H (2007) Fundamentals of biofilm research. CRC Press, Boca Raton
88. Liu H (2001) Transcriptional control of dimorphism in *Candida albicans*. *Curr Opin Microbiol* 4:728–735
89. Minsky M (1988) Memoir on inventing the confocal scanning microscope. *Scanning* 10:128–138
90. Müller M, Zumbusch A (2007) Coherent anti-Stokes Raman scattering microscopy. *Chem Phys Chem* 8:2156–2170
91. Müller S, Nebe-von-Caron G (2010) Functional single-cell analyses: flow cytometry and cell sorting of microbial populations and communities. *FEMS Microbiol Rev* 34:554–587
92. Maamar H, Dubnau D (2005) Bistability in the *Bacillus subtilis* K-state (competence) system requires a positive feedback loop. *Mol Microbiol* 56:615–624
93. Maamar H, Raj A, Dubnau D (2007) Noise in gene expression determines cell fate in *Bacillus subtilis*. *Science* 317:526–529

94. Naumann D, Keller S, Helm D et al (1995) FT-IR spectroscopy and FT-Raman spectroscopy are powerful analytical tools for the non-invasive characterization of intact microbial cells. *J Mol Struct* 347:399–405
95. Neu TR, Walczysko P, Lawrence JR (2004) Two-photon imaging for studying the microbial ecology of biofilm systems. *Microbes Environ* 19:1–6
96. Neu TR, Lawrence JR (2005) One-photon versus two-photon laser scanning microscopy and digital image analysis of microbial biofilms. *Methods Microbiol* 34:89–136
97. Neu TR, Manz B, Volke F et al (2010) Advanced imaging techniques for assessment of structure, composition and function in biofilm systems. *FEMS Microbiol Ecol* 72:1–21
98. Neugebauer U, Rösch P, Schmitt M et al (2006) On the way to nanometer-sized information of the bacterial surface by tip-enhanced Raman spectroscopy. *Chem Phys Chem* 7:1428–1430
99. Neugebauer U, Schmid U, Baumann K et al (2006) Characterization of bacterial growth and the influence of antibiotics by means of UV resonance Raman spectroscopy. *Biopolymers* 82:306–311
100. Neugebauer U, Schmid U, Baumann K et al (2007) Towards a detailed understanding of bacterial metabolism—spectroscopic characterization of *Staphylococcus epidermidis*. *Chem Phys Chem* 8:124–137
101. Newman JR, Ghaemmaghami S, Ihmels J et al (2006) Single-cell proteomic analysis of *S. cerevisiae* reveals the architecture of biological noise. *Nature* 441:840–846
102. Pamp SJ, Gjermansen M, Johansen HK et al (2008) Tolerance to the antimicrobial peptide colistin in *Pseudomonas aeruginosa* biofilms is linked to metabolically active cells, and depends on the pmr and mexAB-oprM genes. *Mol Microbiol* 68:223–240
103. Pamp SJ, Sternberg C, Tolker-Nielsen T (2009) Insight into the microbial multicellular lifestyle via flow-cell technology and confocal microscopy. *Cytometry Part A* 75A: 90–103
104. Patterson GH, Betzig E, Lippincott-Schwartz J et al (2007) Developing Photoactivated Localization Microscopy (PALM). In: 4th IEEE international symposium on biomedical imaging: from nano to macro, ISBI 2007
105. Pavani SRP, Thompson MA, Biteen JS et al (2009) Three-dimensional, single-molecule fluorescence imaging beyond the diffraction limit by using a double-helix point spread function. *Proc Natl Acad Sci USA* 106:2995–2999
106. Pätzold R, Keuntje M, Anders-von Ahlften A (2006) A new approach to non-destructive analysis of biofilms by confocal Raman microscopy. *Anal Bioanal Chem* 386:286–292
107. Radmacher M, Fritz M, Hansma HG et al (1994) Direct observation of enzyme-activity with the atomic-force microscope. *Science* 265:1577–1579
108. Ramage G, Mowat E, Jones B et al (2009) Our current understanding of fungal biofilms. *Crit Rev Microbiol* 35:340–355
109. Reynolds TB, Fink GR (2001) Bakers' yeast, a model for fungal biofilm formation. *Science* 291:878–881
110. Rikkerink EH, Magee BB, Magee PT (1988) Opaque-white phenotype transition: a programmed morphological transition in *Candida albicans*. *J Bacteriol* 170:895–899
111. Rittweger E, Han KY, Irvine SE et al (2009) STED microscopy reveals crystal colour centres with nanometric resolution. *Nat Photon* 3:144–147
112. Robichon D, Girard J-C, Cenatiempo Y et al (1999) Atomic force microscopy imaging of dried or living bacteria. *Comptes Rendus de l'Académie des Sciences - Series III - Sciences de la Vie* 322:687–693
113. Rosch P, Harz M, Schmitt M et al (2005) Chemotaxonomic identification of single bacteria by micro-Raman spectroscopy: application to clean-room-relevant biological contaminations. *Appl Environ Microbiol* 71:1626–1637
114. Ruska E (1987) The development of the electron microscope and of electron microscopy. *Rev Mod Phys* 59:627
115. Rust MJ, Bates M, Zhuang X (2006) Sub-diffraction-limit imaging by stochastic optical reconstruction microscopy (STORM). *Nat Methods* 3:793–796

116. Sandt C, Smith Palmer T, Pink J et al (2008) Quantification of local water and biomass in wild type PA01 biofilms by confocal Raman microspectroscopy. *J Microbiol Methods* 75:148–152
117. Schabert FA, Engel A (1994) Reproducible acquisition of *Escherichia coli* porin surface topographs by atomic force microscopy. *Biophys J* 67:2394–2403
118. Schermelleh L, Carlton PM, Haase S et al (2008) Subdiffraction multicolor imaging of the nuclear periphery with 3D structured illumination microscopy. *Science* 320:1332–1336
119. Schuster KC, Urlaub E, Gapes JR (2000) Single-cell analysis of bacteria by Raman microscopy: spectral information on the chemical composition of cells and on the heterogeneity in a culture. *J Microbiol Methods* 42:29–38
120. Seneviratne CJ, Silva WJ, Jin LJ et al (2009) Architectural analysis, viability assessment and growth kinetics of *Candida albicans* and *Candida glabrata* biofilms. *Arch Oral Biol* 54:1052–1060
121. Shi L, Günther S, Hübschmann T et al (2007) Limits of propidium iodide as a cell viability indicator for environmental bacteria. *Cytometry Part A* 71A: 592–598
122. Shroff H, Galbraith CG, Galbraith JA et al (2007) Dual-color superresolution imaging of genetically expressed probes within individual adhesion complexes. *Proc Natl Acad Sci USA* 104:20308–20313
123. Shtengel G, Galbraith JA, Galbraith CG et al (2009) Interferometric fluorescent super-resolution microscopy resolves 3D cellular ultrastructure. *Proc Natl Acad Sci USA* 106:3125–3130
124. Sil A, Herskowitz I (1996) Identification of asymmetrically localized determinant, Ash1p, required for lineage-specific transcription of the yeast HO gene. *Cell* 84:711–722
125. Slutsky B, Staebell M, Anderson J et al (1987) “White-opaque transition”: a second high-frequency switching system in *Candida albicans*. *J Bacteriol* 169:189–197
126. Smith E, Dent G (2005) Modern Raman spectroscopy: a practical approach. Wiley, New York
127. Smits WK, Eschevins CC, Susanna KA et al (2005) Stripping *Bacillus*: ComK auto-stimulation is responsible for the bistable response in competence development. *Mol Microbiol* 56:604–614
128. Smits WK, Kuipers OP, Veening J-W (2006) Phenotypic variation in bacteria: the role of feedback regulation. *Nat Rev Microbiol* 4:259–271
129. Sprague GF Jr, Blair LC, Thorner J (1983) Cell interactions and regulation of cell type in the yeast *Saccharomyces cerevisiae*. *Annu Rev Microbiol* 37:623–660
130. Sternberg C, Christensen BB, Johansen T et al (1999) Distribution of bacterial growth activity in flow-chamber biofilms. *Appl Environ Microbiol* 65:4108–4117
131. Sternberg C, Tolker-Nielsen T (2006) Growing and analyzing biofilms in flow cells. *Curr Protoc Microbiol* Chapter 1:Unit 1B.2
132. Stoodley P, Sauer K, Davies DG et al (2002) Biofilms as complex differentiated communities. *Annu Rev Microbiol* 56:187–209
133. Thundat T, Allison DP, Warmack RJ et al (1992) Atomic force microscopy of DNA on mica and chemically modified mica. *Scanning Microsc* 6:911–918
134. Thundat T, Allison DP, Warmack RJ et al (1992) Imaging isolated strands of dna-molecules by atomic force microscopy. *Ultramicroscopy* 42:1101–1106
135. Tolker-Nielsen T, Molin S (2000) Spatial organization of microbial biofilm communities. *Microb Ecol* 40:75–84
136. van Sinderen D, Luttinger A, Kong L et al (1995) comK encodes the competence transcription factor, the key regulatory protein for competence development in *Bacillus subtilis*. *Mol Microbiol* 15:455–462
137. Vaziri A, Tang J, Shroff H et al (2008) Multilayer three-dimensional super resolution imaging of thick biological samples. *Proc Natl Acad Sci USA* 105:20221–20226
138. Veening J-W, Smits WK, Hamoen LW et al (2006) Single cell analysis of gene expression patterns of competence development and initiation of sporulation in *Bacillus subtilis* grown on chemically defined media. *J Appl Microbiol* 101:531–541

139. Veening J-W, Stewart EJ, Berngruber TW et al (2008) Bet-hedging and epigenetic inheritance in bacterial cell development. *Proc Natl Acad Sci USA* 105:4393–4398
140. Veening JW, Smits WK, Hamoen LW et al (2004) Visualization of differential gene expression by improved cyan fluorescent protein and yellow fluorescent protein production in *Bacillus subtilis*. *Appl Environ Microbiol* 70:6809–6815
141. Veening JW, Stewart EJ, Berngruber TW et al (2008) Bet-hedging and epigenetic inheritance in bacterial cell development. *Proc Natl Acad Sci USA* 105:4393–4398
142. Vizeacoumar FJ, van Dyk N, Vizeacoumar S et al (2010) Integrating high-throughput genetic interaction mapping and high-content screening to explore yeast spindle morphogenesis. *J Cell Biol* 188:69–81
143. Vlamakis H, Aguilar C, Losick R et al (2008) Control of cell fate by the formation of an architecturally complex bacterial community. *Genes Dev* 22:945–953
144. Wagner M, Ivleva NP, Haisch C et al (2009) Combined use of confocal laser scanning microscopy (CLSM) and Raman microscopy (RM): investigations on EPS-matrix. *Water Res* 43:63–76
145. Wildanger D, Rittweger E, Kastrop L et al (2008) STED microscopy with a supercontinuum laser source. *Opt Express* 16:9614–9621
146. Willig KI, Kellner RR, Medda R et al (2006) Nanoscale resolution in GFP-based microscopy. *Nat Methods* 3:721–723
147. Willig KI, Harke B, Medda R et al (2007) STED microscopy with continuous wave beams. *Nat Methods* 4:915–918
148. Yang L, Liu Y, Sternberg C et al (2010) Evaluation of enoyl-acyl carrier protein reductase inhibitors as *Pseudomonas aeruginosa* quorum-quenching reagents. *Molecules* 15:780–792
149. Yang X, Beyenal H, Harkin G et al (2000) Quantifying biofilm structure using image analysis. *J Microbiol Methods* 39:109–119
150. Zernike F (1935) Das Phasenkontrastverfahren bei der mikroskopischen Beobachtung. *Z Tech Phys* 16:454–457
151. Zipor G, Haim-Vilmsky L, Gelin-Licht R et al (2009) Localization of mRNAs coding for peroxisomal proteins in the yeast, *Saccharomyces cerevisiae*. *Proc Natl Acad Sci USA* 106:19848–19853
152. Zordan RE, Galgoczy DJ, Johnson AD (2006) Epigenetic properties of white-opaque switching in *Candida albicans* are based on a self-sustaining transcriptional feedback loop. *Proc Natl Acad Sci USA* 103:12807–12812
153. Zumbusch A, Holtom GR, Xie XS (1999) Three-dimensional vibrational imaging by coherent anti-Stokes Raman scattering. *Phys Rev Lett* 82:4142

High Resolution Microbial Single Cell Analytics

Müller, S.; Bley, Th. (Eds.)

2011, XIV, 234 p., Hardcover

ISBN: 978-3-642-16886-4